ChemPubSoc Europe

DOI: 10.1002/chem.201603295

CHEMISTRY A European Journal Full Paper

Supramolecular Chemistry

Synthesis of Fluorescent Gelators and Direct Observation of Gelation with a Fluorescence Microscope

Kenji Hanabusa,*[a, b] Takuya Ueda,[a] Shingo Takata,[a] and Masahiro Suzuki[a]

Abstract: Fluorescein-, benzothiazole-, quinoline-, stilbene-, and carbazole-containing fluorescent gelators have been synthesized by connecting gelation-driving segments, including L-isoleucine, L-valine, L-phenylalanine, L-leucine residue, cyclo(L-asparaginyl-L-phenylalanyl), and *trans*-(1*R*,2*R*)-diaminocyclohexane. The emission behaviors of the gelators were investigated, and their gelation abilities studied against 15 solvents. The minimum gel concentration, variable-temperature spectroscopy, transmission electron microscopy, scanning electron microscopy, fluorescence microscopy (FM), and confocal laser scanning microscopy (CLSM) were used to characterize gelation. The intermolecular hydrogen bonding between the N–H and C=O of amide, van der Waals interactions and π–π stacking play important roles in gelation. The colors of emission are related to the fluorescence structures of gelators. Fibrous aggregates characterized by the color of their emission were observed by FM. 3D images are produced by the superposition of images captured by CLSM every 0.1 μm to a settled depth. The 3D images show that the large micrometer-sized aggregates spread out three dimensionally. FM observations of mixed gelators are studied. In the case of gelation, two structurally related gelators with the same gelation-driving segment lead to the gelators build up of the same aggregates through similar hydrogen-bonding patterns. When two gelators with structurally different gelation-driving segments induce gelation, the gelators build up each aggregate through individual hydrogen-bonding patterns. A fluorescent reagent that was incorporated into the aggregates of gels through van der Waals interactions was developed. The addition of this fluorescent reagent enables the successful observation of nonfluorescent gelators' aggregates by FM.

Introduction

In recent years, several researchers have shown considerable interest in studying gelators that can physically gel water or organic solvents. Such gelators are of interest because they can immobilize substantial volumes of solvent. In particular, gelators that can induce gelation when added at masses less than 1 g against 1 L of liquid are called supergelators. Despite the large number of recent papers about gelators in the literature, designing a gelator remains a difficult task. Gelation results from competition between the tendencies for a gelator to dissolve in the solvent and the tendencies for it to crystallize. When a gelator-containing solution is cooled, low-molecular-weight compounds usually give crystals with different solubilities. The first report regarding gelators was published in 1841, when Lipowitz described lithium urate hydorgel.[1] The following report was published in 1942, when Yamamoto described the gelator 1,3:2,4-dibenzylidene-D-sorbitol.[2] Papers on gelators were rare for the next half century; however, research interest increased again during the first half of the 1990s. With advances in the area of supramolecular chemistry, several reports on gelators have been published in recent years.[3–21] Although gelators are of special interest to academic researchers, they also have practical applications. However, the number of gelators used in practical applications remains small. 1,3:2,4-Dibenzylidene-D-sorbitol and *N*-lauroyl-L-glutamate-α,γ-bis-*n*-butylamide are used as ingredients in fragrances and cosmetics, 12-hydroxystearic acid is used as an edible-oil solidifying agent, aromatic diureas are used as ingredients for greases, and aluminum 2-ethylhexanoate, which dissolves at room temperature in hydrocarbon solvents and forms a gel-like viscous product, is used as a thickener for ink.

Several electron microscopy techniques such as SEM, TEM, and AFM have been used to investigate the network structure of the aggregates formed by gelation. Whereas the use of SEM, TEM, and AFM techniques in gelator research is routine, fluorescence microscopy (FM) has not been frequently used because its use is restricted to fluorescent gelators. With respect to the FM technique, Whitten et al. reported FM images of stilbene-containing cholesterol in an octanol gel in 1999.[22] To our knowledge, their work represents the first reported FM images of gels. The application of FM to gelator research has been increasing in recent years, resulting in a limited number of manuscripts.[23–29] Because TEM, SEM, and AFM are limited to the observation of xerogels, they are not applicable to obser-

[a] *Prof. K. Hanabusa, T. Ueda, S. Takata, Prof. M. Suzuki*
Interdisciplinary Graduate School of Science and Technology Shinshu University, Ueda, 386-8567 (Japan)
E-mail: hanaken@shinshu-u.ac.jp

[b] *Prof. K. Hanabusa*
Division of Frontier Fibers, Institute for Fiber Engineering, ICCER Shinshu University, Ueda, 386-8567 (Japan)

Supporting information for this article is available on the WWW under http://dx.doi.org/10.1002/chem.201603295.

vations of wet gels. The observation of real aggregates in wet gels is obviously critical. FM has an advantage in that it enables direct observation of a wet gel containing solvent. Another advantage of FM is that observations are carried out under low magnifications of several hundred times. TEM, SEM, and AFM are effective for observations under high magnifications of several tens of thousands of times. In the case of low-magnification observations, FM is strikingly different from an electron microscopy. Considering that the gelation by low-molecular-weight gelators is a macroscopic expression of molecular self-assembly, FM is well suited to observe large micrometer-sized aggregates.

We herein report the synthesis of various fluorescent gelators by connecting typical gelation-driving segments and the measurement of the gels' fibrous aggregates by TEM, SEM, and FM. In particular, we focused on observation using FM. We clarified the location of each gelator in networks by observing each emission from the formed gels by mixing two different gelators. We also mention a simple fluorescent reagent, which enables the successful observation of aggregates of nonfluorescent gelators in FM.

Results and Discussion

Gelation abilities

Fluorescein-containing gelators (**2**–**5**) were prepared from fluorescein and the corresponding gelation-driving segments by Williamson synthesis (Figure 1). Gelators **2**, **4**, and **5** have L-isoleucine, L-valine, and L-phenylalanine residues in their gelation-driving segments, respectively. Meanwhile, gelator **3** is a dipeptide type, in which L-isoleucyl–L-isoleucyl units are embedded as a gelation-driving segment.

Gelation tests were carried out using the upside-down test-tube method. The results of gelation tests of **2**–**5** against 15 solvents are summarized in Table 1. All compounds **2**–**5** were too soluble in THF and chloroform to act as gelators; by contrast, they were sparingly soluble in hexane, dodecane, and acetonitrile. Compound **2** was the best gelator among **2**–**5** with respect to the number of solvents gelled and the MGCs. Compound **5**, containing L-phenylalanine residue as the gelation-driving segment, gave a precipitate in methanol, 1-propanol, and DMF. This result suggests that L-phenylalanine residue is not useful as a gelation-driving segment. As will be described later, a main driving force for the gelation for our gelators is hydrogen bonding; therefore, we expected compound **3**, which includes an L-isoleucyl–L-isoleucyl unit, to exhibit a strong gelation ability.[30] Contrary to our expectations, compound **3** gave precipitates in cyclohexane, acetone, ethyl ace-

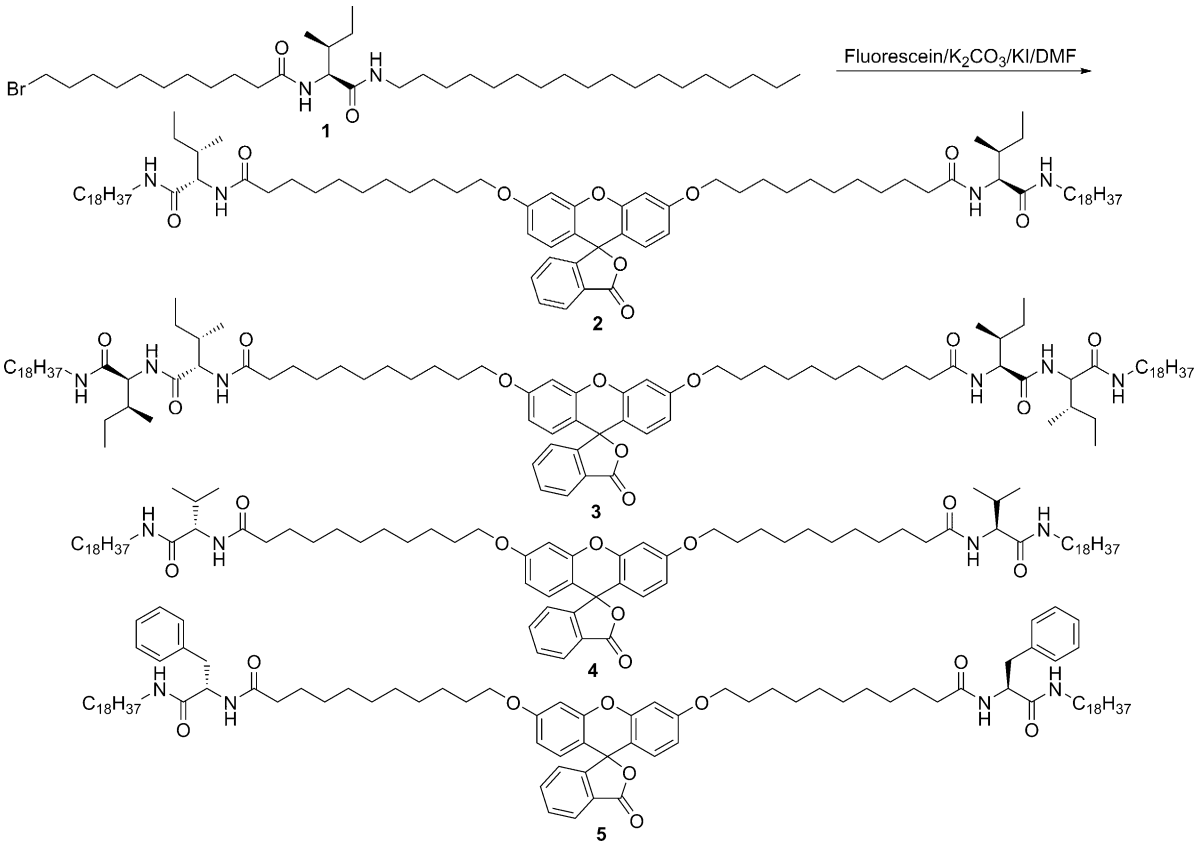

Figure 1. Structure of gelator **1** and fluorescein-containing fluorescent gelators **2**–**5**.

Table 1. Gelation tests of fluorescent gelators **2**–**5** at 25 °C.[a]

Solvent	2	3	4	5
hexane	I	I	I	I
dodecane	I	I	I	I
cyclohexane	GTL(8)	P	GT(8)	GO(20)
methanol	GO(10)	GO(20)	P	P
ethanol	GO(10)	GO(20)	P	GO(40)
1-propanol	GO(10)	GO(20)	GO(20)	P
acetone	GO(20)	P	P	GO(20)
ethyl acetate	GO(20)	P	GO(20)	GO(20)
THF	S	S	S	S
DMF	GTL(8)	GTL(8)	GO(10)	P
DMSO	GTL(8)	GTL(8)	GO(40)	VS
γ-butyrolactone	GTL(8)	GO(20)	GO(20)	GO(40)
toluene	GO(10)	GT(8)	GT(20)	GTL(20)
acetonitrile	I	I	I	I
chloroform	S	S	S	S

[a] GT: transparent gel, GTL: translucent gel, GO: opaque gel, S: soluble, I: almost insoluble, VS: viscous solution. The values indicate the minimum gel concentrations at 25 °C; the units are g L^{-1} (gelator per solvent).

tate, and THF instead of gels. The crystallinity of **3** may arise from the absence of an appropriate hydrophile-lipophile balance. The balance between gelation and crystallization is clearly delicate.

Fluorescent gelators (**6**–**12**) were prepared by Williamson synthesis or by a coupling reaction with the corresponding gelation-driving segments (Figure 2). The results of gelation tests of **6**–**12** are summarized in Table 2. The compounds **6**, **9**, and **10** have benzothiazole as fluorescent segments. Compounds **7** and **8** possess quinoline and stilbene, respectively. Both **11** and **12** have carbazole as fluorescent segments. All compounds in Table 2 were miscible in THF and chloroform. By contrast, they were almost insoluble in hexane and precipitated as crystals from acetone and acetonitrile. The gelators **9** and **10**, which included *trans*-(1*R*,2*R*)-diaminocyclohexane and cyclo(L-asparaginyl-L-phenylalanyl), could gel certain solvents such as 1-propanol and toluene. The gelators **6**, **7**, **11**, and **12** could gel a wide variety of solvents that range from nonpolar to polar solvents and include both protic and aprotic ones. The strong gelation abilities of these gelators suggest that L-isoleucine and L-leucine residues are effective gelation-driving segments.

Variable-temperature spectroscopy

To ensure the participation of hydrogen bonding in physical gelation, we collected variable-temperature IR spectra. IR spectra of the DMSO gel (8 mg mL^{-1}) of **2** collected over the range from 30 to 80 °C is shown in Figure 3; the νN–H of amide I, νC–H of methylene, νC=O of amide I, and δN–H of amide II are evident in these spectra. The DMSO gel at 30 °C was gradually changed to the solution upon heating; specifically, the gel almost collapsed at 50 °C and the isotropic solution was visually observed to have formed at temperatures above 60 °C. The νN–H (amide I), νC–H (methylene), and νC=O (amide I) peaks were shifted by 7, 2, and 9 cm^{-1} toward higher frequencies with increasing temperature, respectively. By contrast, the peak of δN–H (amide II) was shifted toward lower frequencies, from 1595 to 1598 cm^{-1}, with increasing temperature. These observed frequency shifts indicate the transition from an association-type gel to a nonassociation-type gel with increasing temperature. These results led us to conclude that the hydrogen bonding between N–H and C=O of amide and van der Waals interactions are the main driving forces for molecular aggregation to create a network structure for gel formation.

To study the existence of π–π stacking among fluorescein segments, we collected visible spectra of the DMSO gel (4 mg mL^{-1}) of **2** at 30 and 80 °C. The maximum absorption wavelength of 462 nm at 80 °C was blueshifted to 460 nm at 30 °C. This blueshift suggests the existence of π–π stacking similar to that of a J-aggregate in the DMSO gel of **2**.

Table 2. Gelation tests of fluorescent gelators **6**–**12** at 25 °C.[a]

Solvent	6	7	8	9	10	11	12
hexane	I	I	I	I	I	I	GTL(10)
dodecane	GO(20)	GO(20)	GO(40)	I	I	GO(20)	GTL(20)
cyclohexane	GT(20)	GT(20)	I	P	P	GT(20)	GTL(20)
methanol	GO(40)	GO(20)	P	P	P	GO(20)	GO(10)
ethanol	GO(40)	GO(20)	GO(40)	P	GO(40)	GO(20)	GO(10)
1-propanol	GO(40)	GO(40)	GO(40)	GO(40)	GO(40)	GTL(20)	GO(20)
acetone	P	P	P	P	S	P	P
ethyl acetate	GO(40)	GO (40)	P	GO(10)	GO(40)	GO(20)	GTL(20)
THF	S	S	S	S	S	S	S
DMF	GO(40)	GO(10)	GO(40)	P	S	GO(10)	GO(20)
DMSO	GO(40)	GO(10)	GO(40)	GO(40)	S	GO(10)	GO(20)
γ-butyrolactone	GO(40)	GO(10)	GO(40)	P	S	GO(10)	GO(10)
toluene	GT(40)	GT(20)	GTL(10)	GT(40)	GO(40)	GT(40)	S
acetonitrile	P	P	I	P	P	P	GO(10)
chloroform	S	S	S	S	S	S	S

[a] GT: transparent gel, GTL: translucent gel, GO: opaque gel, S: soluble, I: almost insoluble. The values indicate the minimum gel concentrations at 25 °C; the units are g L^{-1} (gelator per solvent).

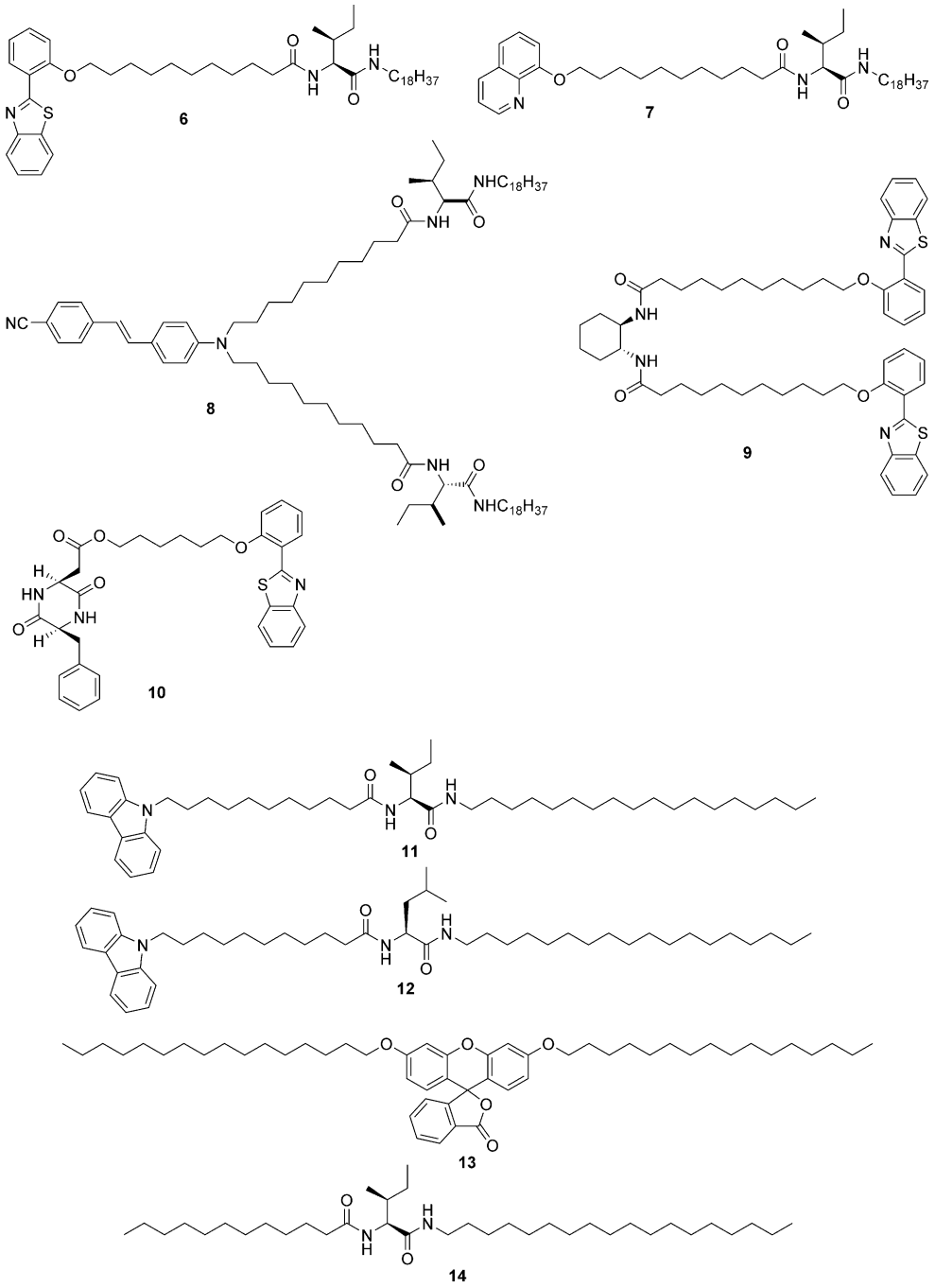

Figure 2. Structure of fluorescent gelators **6**–**12** and compounds **13** and **14**.

TEM studies

Figure 4 shows TEM images of xerogels of fluorescent gelators **2**, **3**, **4**, **6**, **7**, **9**, and **10**, which were prepared from the corresponding loose gels at a concentration of 2 mg mL^{-1}. The xerogels prepared from DMSO loose gels of **2** and **3** exhibited steric networks of juxtaposed, interlocked, and close fibers with nearly homogeneous diameters. Given that the MGCs of **2** and **3** for DMSO were very low (8 mg mL^{-1}), the homogeneous dense fibers are a consequence of the steric networks' effective construction. The xerogel of **9** in ethyl acetate loose gel exhibited thick and short fibers with widths of several hundreds of nanometers. Notably, the ethyl acetate gel of **9** precipitated as crystals after standing for several hours. The ethyl acetate gel instability of **9** is attributed to its thick and short fibers. Xerogel of **10** in ethanol loose gel also contained thick and short fibers the entanglement of which was gentle. The relatively high MGC (40 mg mL^{-1}) of **10** against ethanol may result from the sparsely juxtaposed and interlocked fibers.

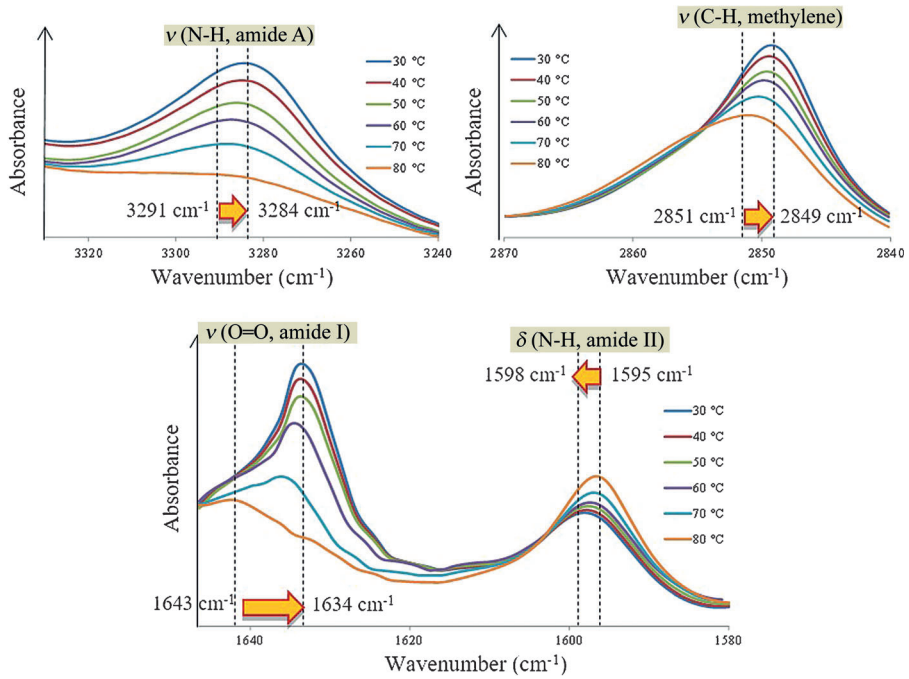

Figure 3. VT-IR spectra of **2** in DMSO gel at 30–80 °C. [**2**] = 8 mg mL^{-1}.

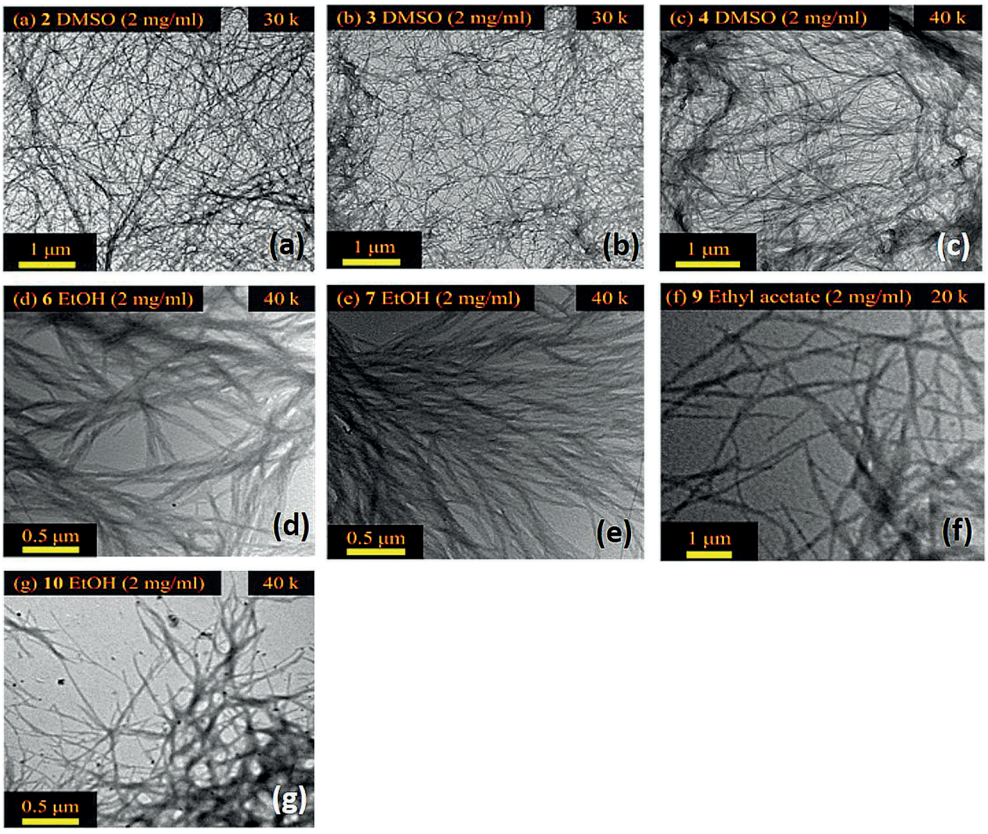

Figure 4. TEM images of xerogels: a) DMSO gel of **2** (2 mg mL^{-1}), b) DMSO gel of **3** (2 mg mL^{-1}), c) DMSO gel of **4** (2 mg mL^{-1}), d) EtOH gel of **6** (2 mg mL^{-1}), e) EtOH gel of **7** (2 mg mL^{-1}), f) ethyl acetate gel of **9** (2 mg mL^{-1}), g) EtOH gel of **10** (2 mg mL^{-1}).

FM studies

For observations by TEM and SEM, dry samples must be prepared. However, the observation of real aggregates in wet gels, excluding xerogels, is important. FM has an advantage that we can directly observe a wet gel containing a solvent. Figure 5 shows FM 2D images of fluorescent gelators (**3**, **5**, **7**, **8**, **9**, and **11**). Figure 5a and b are the FM images of the DMSO gel of fluorescein-containing **3** and the ethanol gel of fluorescein-containing **5**, the images of which are characterized by yellow light emission. Figure 5c, d, e, and f show FM images of the ethanol gel of **7**, toluene gel of **8**, ethyl acetate gel of **9**, and the ethanol gel of **11**, respectively. The quinoline-containing **7**, stilbene-containing **8**, benzothiazole-containing **9**, and carbazole-containing **11** emitted blue, green, blue, and light-blue light, respectively. The emissions are generated from the corresponding fluorescent segments in the aggregates. The dark areas indicate locations at which solvent molecules are trapped. The observed micrometer-sized aggregates in FM are likely more realistic images of gels compared to TEM images of xerogels. Patterns of entanglement among fibrous aggregates were classified either as a bundle form or as a web form resembling the webs spun by spiders, depending on the gelators and solvents. For example, the images in Figure 5a, b, and d show bundle forms, whereas those in Figure 5c, e, and f show web forms. In particular, the structures of gelation-driving segments may play an important role in the patterns of entanglement. The present results are considered sufficient to demonstrate the usefulness of FM in characterizing fluorescent gelators.

Morphological changes during cooling and heating processes were also studied by FM. Figure 6 shows FM images of the DMSO gel (4 mg mL^{-1}) of fluorescein-containing **2** upon cooling. The image immediately collected after the samples were heated showed yellow light emitted obscurely as a whole (Figure 6a), where no aggregates could be observed. This lack of aggregates is why the sample immediately after heating is still a homogeneous solution. When the sample was rapidly cooled to room temperature, partial fibrous aggregates appeared 8 s later (Figure 6b). The aggregates gradually grew and spread out approximately 3 min later (Figure 6c). The aggregates entangled and radially expanded; they were clearly observed approximately 9 min later (Figure 6d), by which time the gelation had completed. By contrast, during the heating process, the aggregates suddenly drifted away 80 s later and the flowing aggregates disappeared 210 s later. This observation indicates that the collapse of the gels begins with disentanglement.

Observation of 3D structure by CLSM

The 3D structure of the DMSO gel (4 mg mL^{-1}) of fluorescein-containing **2** was observed by CLSM. The elucidation of the network structure in gels with CLSM techniques as described here is, as far as we know, unprecedented. The side-view of Präparat is shown in Figure 7a. We focused on points 1 and 2, which have different thicknesses, and carried out 3D observations. The 2D images of the arbitrary depth at points 1 and 2

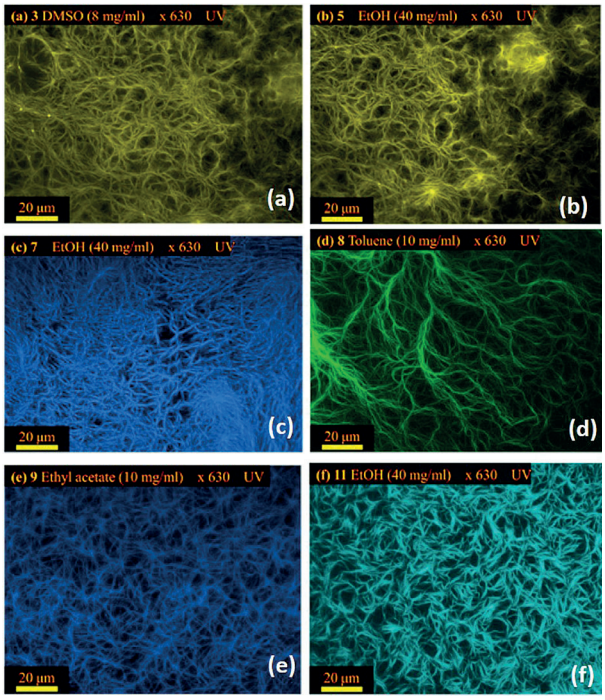

Figure 5. FM images of gels: a) **3** in DMSO gel (8 mg mL^{-1}), b) **5** in EtOH gel (40 mg mL^{-1}), c) **7** in EtOH gel (40 mg mL^{-1}), d) **8** in toluene gel (10 mg mL^{-1}), e) **9** in ethyl acetate gel (10 mg mL^{-1}), f) **11** in EtOH gel (40 mg mL^{-1}).

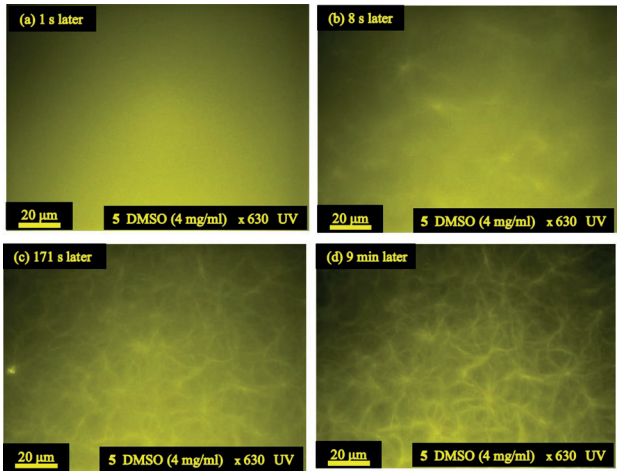

Figure 6. FM images of **2** in DMSO (4 mg mL^{-1}): a) immediately after heating, b) after standing for 8 s, c) after standing for 170 s, d) after standing for 9 min.

are shown in Figure 7b and c, respectively. The image at point 1 is characterized by the entanglement of many fibrous aggregates; however, this image is partially out of focus and was affected by the emission from **2** dissolved in DMSO (Figure 7b). By contrast, fibrous aggregates were clearly observed at point 2 (Figure 7c).

We next constructed 3D images of points 1 and 2. This technique is the similar to the one when CLSM is used for cell imaging, called z-stacking.[31,32] Images were collected every 0.1 μm to a depth of 80 μm at point 1, resulting in a total of

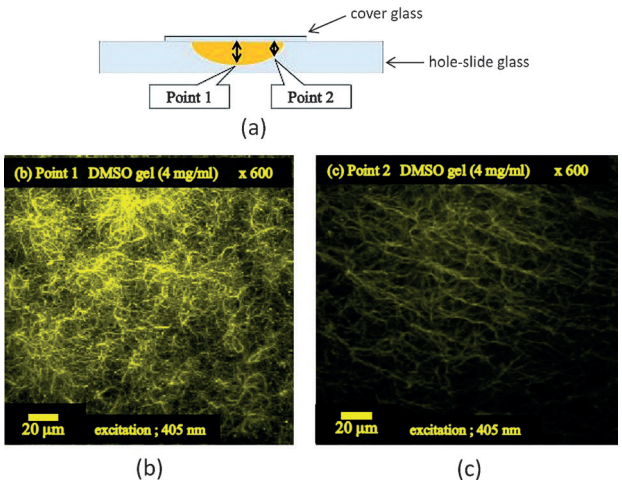

Figure 7. Illustration of Präparat for CSLM and images: a) Präparat indication point 1 and 2, b) CSLM image of DMSO gel of **2** at point 1, c) CSLM image of DMSO gel of **2** at point 2.

800 images, and a total of 90 images were taken at 0.1 μm intervals to a depth of 9 μm at point 2. The obtained 3D images of a 200×200 μm area are shown in Figure 8. In the 3D image at point 1, numerous dense fibrous aggregates were observed and the emission was intense (Figure 8a). Even though the 2D images were collected every 0.1 μm, the obtained 3D image at point 1 was blurred. The result is best interpreted by the existence of numerous fibrous aggregates that spread out three-dimensionally over a depth of 80 μm at point 1. Consequently, the emission from fluorescein outside the observation range was also detected. At point 2, where images were taken every 0.1 μm to a depth of 9 μm, the 3D image was clear (Figure 8b).

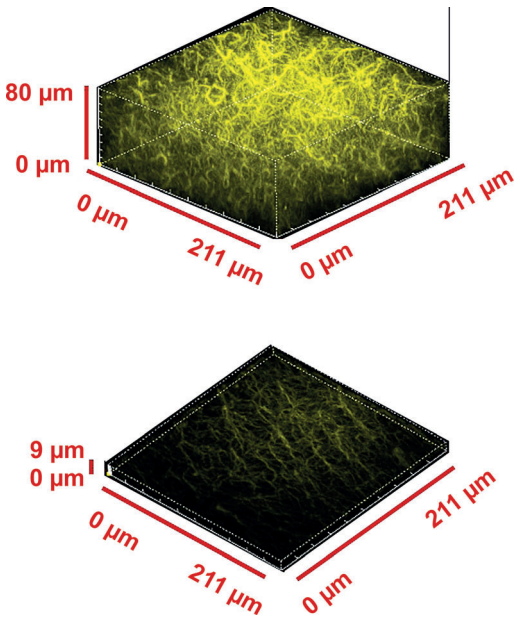

Figure 8. The 3D images of a 200 mm square prepared by superposition of CSLM images at the point 1 (above) and point 2 (below).

The obtained clear 3D image is attributed to the exclusion emissions outside the observation range. Given the combined CLSM results, we concluded that the large micrometer-size aggregates, which were observed in the 2D FM images, spread out three-dimensionally and that the resulting 3D networks trap solvents in space, finally inducing gelation.

FM images of two-component gelators

When gels are formed by the addition of structurally different gelators, a question arises as to whether they are disorderly incorporated into fibrous aggregates or form their respective aggregates separately. To answer this question, we focused on gels formed by the combination of two gelators. One of the two-component gelator systems is a combination of gelator **1** and carbazole-containing gelator **11**, which includes the same gelation-driving segment of L-isoleucine. The other system is a combination of fluorescein-containing gelator **2** and benzothiazole-containing gelator **10**, which includes substantially different gelation-driving segments.

Figure S1a, in the Supporting Information, shows the FM 2D image of an ethanol solution (4 mg mL^{-1}) of **11**, and Figure S1b shows an ethanol gel prepared from the mixture of **1** (36 mg mL^{-1}) and **11** (4 mg mL^{-1}). The FM 2D image of the ethanol gel (40 mg mL^{-1}) of **11** was characterized by light-blue emission from bundled aggregates (Figure 5e). Given the lack of a fluorescent segment in **1**, the FM image of **1** was a dark field. The ethanol solution (4 mg mL^{-1}) of **11** also gave an almost dark-field image because the gel failed to form when the concentration of **11** was 4 mg mL^{-1}, which is substantially less than the MGC (Figure S1a). Aggregates that emitted light-blue light were observed in the FM image of the ethanol gel of **1** containing a small amount of **11** (Figure S1b). Because the gelator **1** emits no light, we assumed that the fluorescent gelator **11** was disorderly incorporated into fibrous aggregates of **1**. When gels are formed by two structurally related gelators with the same gelation-driving segment, the gelators conceivably build up the same aggregates through a similar hydrogen-bonding pattern.

We next studied gels prepared from the mixture of fluorescein-containing gelator **2** and benzothiazole-containing gelator **10**, which include L-isoleucine residue and cyclo(L-asparaginyl-L-phenylalanyl) as gelation-driving segments, respectively. The FM image in Figure 9a was due to the UV excitation of benzothiazole-containing gelator **10**. Although the fluorescein-containing gelator **2** simultaneously emits yellow under UV excitation, this yellow emission was cut off by the fluorescence filter in the case of Figure 9a. Figure 9b shows the image obtained by G excitation, which was obtained by observing the location of the same Präparat of Figure 9a. Because no fluorescence was observed from the benzothiazole-containing gelator **10** under G excitation, the yellow emission in Figure 9b was caused from the fluorescein-containing gelator **2**. Figure 9c was constructed by overlaying two images. Figure 9c indicates that the aggregates, which emitted light-blue and yellow light, are separately present from each other. That is, gelators **2** and **10** separately form their respective network structures in the

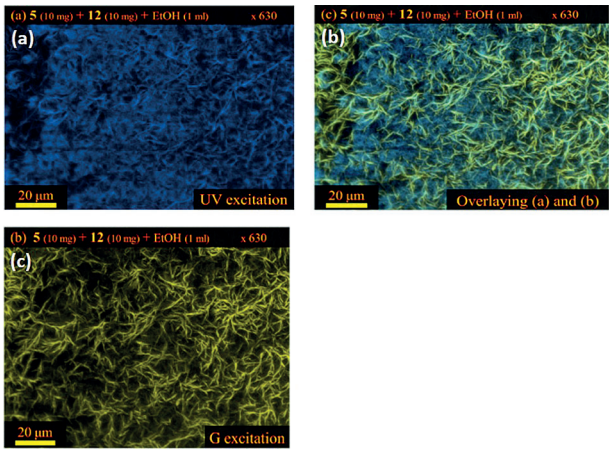

Figure 9. FM images of EtOH gels from two-component gelators **2** (10 mg mL^{-1}) and **10** (10 mg mL^{-1}): a) image by UV excitation, b) image by G excitation, c) image constructed by overlaying two images.

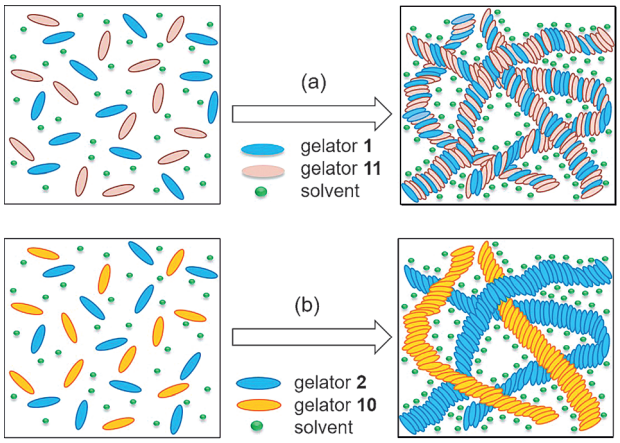

Figure 10. Illustration of the gelation process by two-component gelators: a) gelation process by two structurally related gelators including the same gelation-driving segment, b) gelation process by two gelators with structurally different gelation-driving segments.

gel. We conclude that when two gelators with structurally different gelation-driving segments cause gelation, the gelators build up each aggregate through individual hydrogen-bonding patterns.

The fact that structurally different gelators build up each micrometer-sized aggregate in gels was also confirmed by FE-SEM and TEM (Figure S2, Supporting Information). FE-SEM and TEM images of the benzothiazole-containing gelator **10** were characterized by aggregates comprising short fibers (Figure S2a and b), whereas images of the fluorescein-containing gelator **2** were characterized by bundle aggregates (Figure S2c and d). In the FE-SEM and TEM images of two-component xerogels prepared from the mixture of **2** and **10**, different aggregates, each with its own aggregate characteristics, were observed (Figure S2e and f). These results suggest that gelators **2** and **10** separately form their respective nanometer-sized aggregates in the early stage of gelation and then simultaneously but separately grow into their respective aggregates, which are the large micrometer-sized aggregates observed by FM.

On the basis of the results of gelation by two-component gelators, we illustrate the gelation processes as shown in Figure 10. In the case of gelation by two structurally related gelators including the same gelation-driving segment, the gelators build up the same aggregates through similar hydrogen-bonding patterns (Figure 10a). When two gelators with structurally different gelation-driving segments cause gelation, the gelators build up each aggregate through individual hydrogen-bonding patterns (Figure 10b).

Fluorescent reagent for FM

Gelators do not always include fluorescence segments, and FM is not applicable to nonfluorescent gelators. To observe aggregates of nonfluorescent gelators using FM, we prepared fluorescent reagent **13**. That is, the fluorescent reagent that we propose here is thought to act like osmium tetroxide as a negative staining reagent in the preparation of TEM samples. We collected FM images of gelator **14** in the presence of fluorescent reagent **13**. Notably, gelator **14** could gel ordinary solvents, but not emit under UV excitation. Figure 11 shows CLSM images of a 1-propanol gel (20 mg mL^{-1}) and a DMSO gel (10 mg mL^{-1}) of **14**; these gels contain 1 mg of fluorescent reagent **13**. The 1-propanol and DMSO gels of **14** exhibit steric networks of close fibers and thick fibers that emit yellow light because of the presence of **13**. Neither clusters nor precipitates of **13** were observed in the images. Because fluorescent reagent **13** has no hydrogen-bonding sites, we assumed that **13** would be incorporated into the aggregates of **14** through van der Waals interactions among long alkyl groups. Compound **13** will be very useful as a fluorescent reagent for FM observations because most gelators have long alkyl chains.

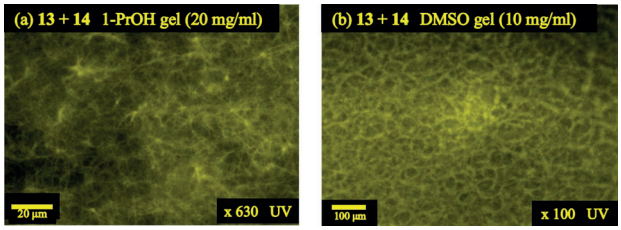

Figure 11. CSLM images of **1**-PrOH gel (20 mg mL^{-1}) and DMSO gel (10 mg mL^{-1}) of **14**, which are contain 1 mg of fluorescent reagent **13**.

Conclusions

We prepared fluorescein, benzothiazole, quinoline, stilbene, and carbazole-containing fluorescent gelators by connecting typical gelation-driving segments. The gelators, including L-isoleucine or L-leucine residue as gelation-driving segments, showed strong gelation abilities. Close fibers with nearly homogeneous diameters were observed in TEM images of gels formed by gelators with low MGCs. Variable-temperature IR spectra suggested that the hydrogen bonding between the N–H and C=O of amide and van der Waals interactions are im-

portant main driving forces of gelation. By FM observation, we directly observed the fibrous aggregates in wet gel containing solvents. The 3D images, which were produced by the superposition of images taken by CLSM every 0.1 μm to a settled depth, suggested that the large micrometer-sized aggregates spread out three-dimensionally and that the resulting 3D network traps solvents in the space, finally inducing gelation. FM observations of mixed gelators gave two conclusions. When gels are formed by two structurally related gelators with the same gelation-driving segment, the gelators build up the same aggregates through similar hydrogen-bonding patterns. By contrast, when two gelators including structurally different gelation-driving segments cause gelation, the gelators build up each aggregate through individual hydrogen-bonding patterns. We developed a simple fluorescent reagent, that is, a fluorescein derivative with two long alkyl chains. The addition of this fluorescent reagent enabled the successful observation of aggregates of nonfluorescent gelators by FM. Because this fluorescent reagent is incorporated into the aggregates of gels through van der Waals interactions, it may be useful as a fluorescent reagent for FM observations.

Experimental Section

Instrumentation

Elemental analysis was performed with a Perkin–Elmer 240B analyzer. IR spectra were recorded on a Jasco FTIR-7300 spectrometer by using a KBr plate. TEM and field-emission SEM (FE-SEM) were done with a JEOL JEM-SS and a Hitachi S-5000, respectively. ^{1}H NMR spectra were taken in $CDCl_3$ on a Bruker AVANCE 400 spectrometer and the chemical shifts were recorded in ppm (δ) downfield from TMS. UV/Vis and fluorescence spectra were recorded on a Jasco V-570UV/VIS/NIR and a Jasco FP-6300. FM and confocal laser scanning microscopy (CLSM) were performed with a Carl Zeiss Axio Imager M1 and an Olympus FV1000-D, respectively.

Synthesis of fluorescent gelators

Fluorescent gelator 2: A mixture of 0.66 g (2.0 mmol) of fluorescein, 0.44 g (3.2 mmol) of potassium carbonate, 0.33 g (2.0 mmol) of potassium iodide, 2.77 g (4.4 mmol) of *N*-11-bromoundecanoyl-L-isoleucylaminooctadecane (**1**),[33] and 70 mL of dry DMF was stirred at 50 °C overnight under an argon atmosphere. The mixture was poured to iced water and the precipitated matter was filtered off, washed with water, and dried. The crude product obtained was purified by column chromatography on alumina (elution with chloroform/methanol = 9:1; R_f = 0.9). Fluorescent gelator **2** was obtained by recrystallization from ethyl acetate in a yield of 2.03 g (71 %). IR (KBr): $\tilde{\nu}$ = 3288 (νNH amide A), 1727 (νC=O lactone), 1637 cm^{-1} (νC=O amide I), 1545 cm^{-1} (δN–H amide II); elemental analysis calcd (%) for $C_{90}H_{148}N_4O_9$: calcd for C 75.58, H 10.43, N 3.92; found: C 75.20, H 10.57, N 3.79; excitation maximum: 381 nm; emission maximum: 547 nm (chloroform).

Fluorescent gelator 3: *N*-Benzyloxycarbonyl-L-isoleucyl-L-isoleucylaminooctadecane[30] (31.5 g, 50 mmol) was hydrogenated in the presence of Pd/C in 300 mL of 1-propanol for 5 h. After confirming the complete removal of protecting group by TLC, the solution was filtered off. The filtrate was evaporated and recrystallization from 200 mL of ligroin provided 22.3 g (90 %) of L-isoleucyl-L-isoleucylaminooctadecane. A solution of 9.92 g (20 mmol) of L-isoleucyl-L-isoleucylaminooctadecane and 5.4 mL (40 mmol) of triethylamine in 300 mL of dry THF was cooled in an ice/water bath, and then 6.24 g (22 mmol) of 11-bromoundecanoyl chloride was added drop-by-drop. The matter was stirred for 1 h in ice/water bath, followed by for 4 h at room temperature. A filtrate without NEt_3/HCl salt was evaporated and recrystallized from 1-propanol. *N*-11-Bromoundecanoyl-L-isoleucyl-L-isoleucylaminooctadecane was obtained in a yield of 14.0 g (96 %). Fluorescent gelator **3** was obtained from a mixture of 0.66 g (2.0 mmol) of fluorescein, 0.44 g (3.2 mmol) of potassium carbonate, 0.33 g (2.0 mmol) of potassium iodide, 3.21 g (4.4 mmol) of *N*-11-bromoundecanoyl-L-isoleucyl-L-isoleucylaminooctadecane, and 50 mL of dry DMF by the similar procedure described in gelator **2**. An obtained crude product was purified by column chromatography on alumina (elution with chloroform/methanol = 9:1; R_f = 0.9). The fluorescent gelator **3** was obtained by recrystallization from ethanol/ether in a yield of 2.26 g (69 %). IR (KBr): $\tilde{\nu}$ = 3284 (νNH amide A), 1725 (νC=O lactone), 1633 (νC=O amide I), 1547 cm^{-1} (δN-H amide II); elemental analysis calcd (%) for $C_{102}H_{170}N_6O_{11}$: C 73.96, H 10.34, N 5.07; found: C 73.52, H 10.77, N 5.38; excitation maximum: 382 nm; emission maximum: 546 nm (chloroform).

Fluorescent gelator 4: A solution of 7.37 g (20 mmol) of L-valylaminooctadecane[34] and 5.4 mL (40 mmol) of triethylamine in 400 mL of dry THF was cooled in an ice/water bath, and then 6.24 g (22 mmol) of 11-bromoundecanoyl chloride was added drop-by-drop. The matter was stirred for 1 h in an ice/water bath, followed by for 4 h at room temperature. The recrystallization from ligroin gave *N*-11-bromoundecanoyl-L-valyaminooctadecane in a yield of 10.49 g (85 %). Fluorescent gelator **4** was obtained from a mixture of 0.66 g (2.0 mmol) of fluorescein, 0.44 g (3.2 mmol) of potassium carbonate, 0.33 g (2.0 mmol) of potassium iodide, 2.71 g (4.4 mmol) of *N*-11-bromoundecanoyl-L-valylaminooctadecane, and 50 mL of dry DMF by the similar procedure described in gelator **2**. An obtained crude product was purified by column chromatography on alumina (elution with chloroform/methanol = 9:1; R_f = 0.9). The fluorescent gelator **4** was obtained by recrystallization from ethanol/ether in a yield of 1.85 g (66 %). IR (KBr, cm^{-1}): $\tilde{\nu}$ = 3288 (νNH amide A), 1725 (νC=O lactone), 1634 (νC=O amide I), 1545 cm^{-1} (δN–H amide II); elemental analysis calcd (%) for $C_{89}H_{146}N_4O_9$: C 75.38, H 10.52, N 3.95; found: C 75.12, H 10.65, N 4.05; excitation maximum: 380 nm; emission maximum: 546 nm (chloroform).

Fluorescent gelator 5: Fluorescent gelator **5** was obtained from a mixture of 0.66 g (2.0 mmol) of fluorescein, 0.44 g (3.2 mmol) of potassium carbonate, 0.33 g (2.0 mmol) of potassium iodide, 2.92 g (4.4 mmol) of *N*-11-bromoundecanoyl-L-phenylalanylaminooctadecane, and 50 mL of dry DMF by a similar procedure as that described for gelator **2**. An obtained crude product was purified by column chromatography on alumina (elution with chloroform/methanol = 94:4; R_f = 0.9). The fluorescent gelator **5** was obtained by recrystallization from ethanol/ether in a yield of 2.00 g (67 %). IR (KBr, cm^{-1}): $\tilde{\nu}$ = 3281 (νNH amide A), 1722 (νC=O lactone), 1640 (νC=O amide I), 1548 cm^{-1} (δN–H amide II); elemental analysis calcd (%) for $C_{97}H_{146}N_4O_9$: C 76.94, H 9.85, N 3.70; found: C 76.51 H 9.97, N 3.65; excitation maximum: 381 nm; emission maximum: 546 nm (chloroform).

Fluorescent gelator 6: A mixture of 0.91 g (4.0 mmol) of 2-(2-hydroxyphenyl)benzothiazole, 0.88 g (6.4 mmol) of potassium carbonate, 0.66 g (4.0 mmol) of potassium iodide, 2.77 g (4.4 mmol) of **1**,

and 40 mL of dry DMF was stirred at 50 °C overnight under an argon atmosphere. The mixture was poured into iced water and the precipitated matter was filtered off, washed with water, and dried. A crude product obtained by recrystallization from ethanol was purified by column chromatography on alumina (elution with chloroform; $R_f = 0.85$). The fluorescent gelator **6** was obtained by recrystallization from ethanol in a yield of 2.11 g (68%). IR (KBr): $\tilde{\nu} = 3288$ (νNH amide A), 1634 (νC=O amide I), 1542 (δN–H amide II), 753 cm^{-1} (benzothiazole); ^1H NMR (400 Hz, $CDCl_3$, TMS, 25 °C): $\delta = 5.78$ (t, $J = 5.8$ Hz, 1H; CONHC*H*), 6.00 (d, $J = 8.8$ Hz, 1H; CHCON*H*), 7.04 (m, 2H; 3-Ph*H*, 5-Ph*H*), 7.35–7.50 (m, 3H; 4-Ph*H*, 5, 6-benzothiazole*H*), 7.93 (d, $J = 8.5$ Hz, 1H; 6-Ph*H)*, 8.07 (d, $J = 8.8$ Hz, 1H; 4-benzothiazole*H)*, 8.54 ppm (d, $J = 9.6$ Hz, 1H; 7-benzothiazole*H*); elemental analysis calcd (%) for $C_{48}H_{77}N_3O_3S$: C 74.27, H 10.00, N 5.41; found: C 73.80, H 10.54, N 6.09; excitation maximum: 354 nm; emission maximum: 417 nm (ethanol).

Fluorescent gelator 7: A mixture of 0.29 g (2.0 mmol) of 8-hydroxyquinoline, 0.44 g (3.2 mmol) of potassium carbonate, 0.33 g (2.0 mmol) of potassium iodide, 1.39 g (2.2 mmol) of **1**, and 20 mL of dry DMF was stirred at 50 °C overnight under an argon atmosphere. The mixture was poured into iced water and the precipitated matter was filtered off, washed with water, and dried. A crude product obtained by recrystallization from ethanol was purified by column chromatography on alumina (elution with chloroform; $R_f = 0.7$). The fluorescent gelator **7** was obtained by recrystallization from methanol in a yield of 0.90 g (63%). IR (KBr): $\tilde{\nu} = 3287$ (νNH amide A), 1634 (νC=O amide I), 1541 (δN–H amide II), 820, 789, 745 cm^{-1} (quinoline); elemental analysis calcd (%) for $C_{44}H_{75}N_3O_3$: C 76.14, H 10.89, N 6.05; found: C 75.91, H 10.96, N 6.18; excitation maximum: 358 nm; emission maximum: 415 nm (ethanol).

Fluorescent gelator 8: This compound was obtained by the reaction of **1** and *trans*-4-(4-aminostyrly)benzonitrile according to our previous paper.[33]

Fluorescent gelator 9: A mixture of 1.00 g (4.4 mmol) of 2-(2-hydroxyphenyl)benzothiazole, 0.88 g (6.4 mmol) of potassium carbonate, 0.66 g (4.0 mmol) of potassium iodide, 1.22 g (2.0 mmol) of *trans*-(1*R*,2*R*)-bis(11-bromoundecanoylamino)cyclohexane,[35] and 50 mL of dry DMF was stirred at 50 °C overnight under an argon atmosphere. The mixture was poured to iced water and the precipitated matter was filtered off, washed with water, and dried. A crude product obtained by recrystallization from methanol was purified by column chromatography on silica gel (elution with chloroform; $R_f = 0.65$). The fluorescent gelator **9** was obtained by recrystallization from ethyl acetate/methanol in a yield of 0.87 g (48%); IR (KBr): $\tilde{\nu} = 3285$ (νNH amide A), 1636 (νC=O amide I), 1542 (δN-H amide II), 754 cm^{-1} (benzothiazole); ^1H NMR (400 Hz, $CDCl_3$, TMS, 25 °C): $\delta = 5.99$ (d, $J = 7.0$ Hz, 2H; CH_2CONH), 7.01 (d, $J = 8.3$ Hz, 2H; 3-Ph*H*), 7.08 (t, $J = 7.0$ Hz, 2H; 5-Ph*H*), 7.34–7.50 (m, 6H; 4-Ph*H*, 5,6-benzothiazole*H*), 7.92 (d, $J = 7.7$ Hz, 2H; 6-Ph*H*), 8.06 (d, $J = 8.1$ Hz, 2H; 4-benzothiazole*H*), 8.50 ppm (d, $J = 9.6$ Hz, 2H; 7-benzothiazole*H*); elemental analysis calcd (%) for $C_{54}H_{68}N_4O_4S_2$: C 71.96, H 7.60, N 6.22; found: 70.82, H 7.62, N 6.24; excitation maximum: 354 nm; emission maximum: 418 nm (ethyl acetate).

Fluorescent gelator 10: A mixture of 10.50 g (40 mmol) of cyclo(L-asparaginyl-L-phenylalanyl),[36] 7.24 g (40 mmol) of 6-bromo-1-hexanol, 11.78 g (40 mmol) of DPTS (4-dimethylamino pyridinium *p*-toluenesulfonate), 5.55 g (44 mmol) of DIPC (*N*,*N*′-diisopropylcarbodiimide), and 150 mL of dry DMF was stirred overnight at 35 °C. After evaporating DMF, the residue was dissolved in 200 mL of hot 1-propanol and cooled to room temperature. The formed gel was ground by mechanical stirrer and filtered, followed by drying. 6-Bromohexyloxy-cyclo(L-asparaginyl-L-phenylalanyl) was obtained in a yield of 15.14 g (89%). A mixture of 0.91 g (4.0 mmol) of 2-(2-hydroxyphenyl)benzothiazole, 0.88 g (6.4 mmol) of potassium carbonate, 0.66 g (4.0 mmol) of potassium iodide, 1.70 g (4.0 mmol) of 6-bromohexyloxy-cyclo(L-asparaginyl-L-phenylalanyl), and 40 mL of dry DMF was stirred at 50 °C overnight under an argon atmosphere. The mixture was poured to iced water and the precipitated matter was filtered off, washed with water, and dried. Recrystallization from ethyl acetate gave 1.92 g (84%) of **10**. $R_f = 0.9$ (chloroform/methanol = 9:1, silica gel); IR (KBr): $\tilde{\nu} = 1739$ (νC=O ester), 1673 (νC=O amide I), 755 cm^{-1} (benzothiazole); elemental analysis calcd (%) for $C_{32}H_{33}N_3O_5S$: C 67.23, H 5.82, N 7.35; found: C 65.92, H 5.95, N 7.33; excitation maximum: 351 nm; emission maximum: 434 nm (toluene).

Fluorescent gelator 11: To a solution of 13.54 g (81 mmol) of carbazole and 1.94 g (81 mmol) of NaH in 90 mL of dry DMF, was added 22.61 g (81 mmol) of methyl 11-bromoundecanoate and 0.083 g (0.5 mmol) of potassium iodide. The resulting mixture was stirred at 80 °C overnight under an argon atmosphere. The mixture was poured to iced water and the precipitated matter was filtered off and washed with water. A wet crude product was hydrolyzed in 400 mL of a mixture of acetone, methanol, and water (5:2:3) including 6.48 g (162 mmol) of NaOH at 40 °C overnight. After neutralization by hydrochloric acid, a precipitate was filtered off and dried. A crude product was recrystallization from 100 mL of methanol. The obtained product was further purified by column chromatography on silica gel (elution with chloroform; $R_f = 0.16$). Recrystallization from methanol gave 11-(9*H*-carbazol-9-yl)undecanoic acid in a yield of 14.53 g (51%). A mixture of 7.03 g (20 mmol) of 11-(9*H*-carbazol-9-yl)undecanoic acid, 7.65 g (20 mmol) of L-isoleucylaminooctadecane, 2.28 g (22 mmol) of DIPC, 2.44 g (20 mmol) of DMAP (4-dimethylaminopyridine), and 100 mL of dichloromethane was refluxed overnight. Chloroform (100 mL) was added to the reaction mixture and an insoluble matter was removed. The resulting filtrate was washed with 100 mL of 1 M hydrochloric acid, followed by 100 mL of water and dried. After evaporating, recrystallization from methanol gave 10.04 g (70%) of **11**. $R_f = 0.7$ (chloroform, alumina); IR (KBr): $\tilde{\nu} = 3289$ (νNH amide A), 1634 (νC=O amide I), 748, 719 cm^{-1} (carbazole); elemental analysis calcd (%) for $C_{47}H_{77}N_3O_2$: C 78.83, H 10.84, N 5.87; found: C 77.93, H 11.13, N 5.71; excitation maximum: 405 nm; emission maximum: 482 nm (chloroform).

Fluorescent gelator 12: Fluorescent gelator **12** was obtained from a mixture of 1.76 g (5.0 mmol) of 11-(9*H*-carbazol-9-yl)undecanoic acid, 1.92 g (5.0 mmol) of L-leucylaminooctadecane, 0.70 g (5.5 mmol) of DIPC, 0.61 g (5.0 mmol) of DMAP, and 40 mL of dichloromethane by a similar procedure to that described for gelator **11**. Yield: 1.26 g (35%); $R_f = 0.83$ (chloroform, alumina); IR (KBr): $\tilde{\nu} = 3300$ (νNH amide A), 1635 (νC=O amide I), 1541 (δN–H amide II), 749, 719 cm^{-1} (carbazole); elemental analysis calcd (%) for $C_{47}H_{77}N_3O_2$: C 78.83, H 10.84, N 5.87; found: C 78.23, H 11.11, N 6.27; excitation maximum: 408 nm; emission maximum: 485 nm (chloroform).

Fluorescent gelator 13: A mixture of 1.66 g (5.0 mmol) of fluorescein, 0.56 g (10.0 mmol) of potassium hydroxide, 0.83 g (5.0 mmol) of potassium iodide, 3.36 g (11.0 mmol) of 1-bromohexadecane, and 20 mL of dry DMF was stirred at 50 °C overnight under an argon atmosphere. An obtained crude product was purified by column chromatography on alumina (elution with chloroform; $R_f =$

0.62). The compound **13** was obtained by recrystallization from hexane/methanol in a yield of 2.43 g (62%). IR (KBr): $\tilde{\nu}=2920$, 2851 (νCH_2), 1718 ($\nu C{=}O$ lactone), 1603, 1286, 1254 cm^{-1}; elemental analysis calcd (%) for $C_{52}H_{76}O_5$: C 79.95, H 9.81; found: C 79.14, H 10.37; excitation maximum: 380 nm; emission maximum: 547 nm (chloroform).

Compound 14: This compound was prepared from 7.65 g (20 mmol) of L-isoleucylaminooctadecane, 4.38 g (20 mmol) of *n*-dodecanoy chloride, 5.4 mL (40 mmol) of triethylamine, and 300 mL of dry THF by a similar procedure to that described for gelator **3**. A crude product was dissolved in hot ethyl acetate and cooled to room temperature. The formed gel was ground by mechanical stirrer and filtered, followed by drying. Yield: 10.17 g (90%); IR (KBr): $\tilde{\nu}=3288$ (νNH amide A), 1634 ($\nu C{=}O$ amide I), 1542 cm^{-1} (δN–H amide II); elemental analysis calcd (%) for $C_{35}H_{69}BrN_2O_2$: C 76.53, H 12.85, N 4.97; found: C 76.44, H 12.65, N 5.12.

Gelation test

A gelation test was performed by the upside-down testtube method. A weighed sample and 1 mL of solvent in a septum-capped test tube with internal diameter of 14 mm was heated until the solid dissolved. The resulting solution was cooled at 25 °C for 2 h and then the gelation was checked visually. When no fluid ran down the wall of the test tube upon inversion of the test tube, we judged it to be gel. The gelation ability was estimated by the minimum gel concentration (MGC), which is the minimum concentration of a gelator necessary for gelation at 25 °C. The unit is g L^{-1} (gelator per solvent).

Sample preparation for TEM

For the TEM samples, fluorescent gelators were dissolved in solvents at the concentration of 2 mg mL^{-1}, and a droplet of the solution was placed on MICA-coated grid (copper, 400 mesh). The solvent was evaporated spontaneously at room temperature for 2 h, and then dried by a vacuum pump overnight. The samples were negatively stained with osmium tetroxide vapor (2 wt% acetone solution) for 10 h.

Sample preparation for FE-SEM

Fluorescent gelators were dissolved in solvents at the MGC and a droplet of the hot solution was placed on a sample table. The solvent was evaporated spontaneously at room temperature for 2 h, and then dried by a vacuum pomp overnight. The sample table was shadowed to approximately 10 nm thickness with Pt by a Hitachi ion sputtering apparatus E-1010.

Sample preparation for FM and CLSM

For the prepared specimens, fluorescent gelators were dissolved in solvents at the MGC and a few droplets of the hot solution were placed on a hole-slide glass, and then a cover glass was put on the hole-slide glass.

Acknowledgements

The present research was supported in part by a Grant-in-Aid for Scientific Research (C) (No. 15K05623) from the Ministry of Education, Culture, Sports, Science and Technology of Japan.

Keywords: fluorescence · fluorescence microscopy · gels · gelation · gelators

[1] A. V. Lipowitz, *Liebigs Ann.* **1841**, *38*, 348.
[2] S. Yamamoto, *J. Chem. Soc. Jpn. Ind. Chem. Soc.* **1943**, *46*, 779; *Chem. Abstr.* **1952**, *46*, 7047i.
[3] P. Terech, R. G. Weiss, *Chem. Rev.* **1997**, *97*, 3133.
[4] J. H. van Esch, B. L. Feringa, *Angew. Chem. Int. Ed.* **2000**, *39*, 2263; *Angew. Chem.* **2000**, *112*, 2351.
[5] L. A. Estroff, A. D. Hamilton, *Chem. Rev.* **2004**, *104*, 1201.
[6] P. Dastidar, *Chem. Soc. Rev.* **2008**, *37*, 2699.
[7] S. Banerjee, R. K. Das, U. Maitra, *J. Mater. Chem.* **2009**, *19*, 6649.
[8] M. Suzuki, K. Hanabusa, *Chem. Soc. Rev.* **2009**, *38*, 967.
[9] M. Suzuki, K. Hanabusa, *Chem. Soc. Rev.* **2010**, *39*, 455.
[10] J.-L. Li, X.-Y. Liu, *Adv. Funct. Mater.* **2010**, *20*, 3196.
[11] G. John, B. V. Shankar, S. R. Jadhav, P. K. Vemula, *Langmuir* **2010**, *26*, 17843.
[12] H. Svobodová, V. Noponen, E. Kolehmainen, E. Sievänen, *RSC Adv.* **2012**, *2*, 4985.
[13] S. S. Babu, S. Prasanthkumar, A. Ajayaghosh, *Angew. Chem. Int. Ed.* **2012**, *51*, 1766; *Angew. Chem.* **2012**, *124*, 1800.
[14] A. Y.-Y. Tam, V. W.-W. Yam, *Chem. Soc. Rev.* **2013**, *42*, 1540.
[15] J. Raeburn, A. Z. Cardoso, D. J. Adams, *Chem. Soc. Rev.* **2013**, *42*, 5143.
[16] G. Yu, X. Yan, C. Han, F. Huang, *Chem. Soc. Rev.* **2013**, *42*, 6697.
[17] M. D. Segarra-Maset, V. J. Nebot, J. F. Miravet, B. Escuder, *Chem. Soc. Rev.* **2013**, *42*, 7086.
[18] S. S. Babu, V. K. Praveen, A. Ajayaghosh, *Chem. Rev.* **2014**, *114*, 1973.
[19] D. K. Kumar, J. W. Steed, *Chem. Soc. Rev.* **2014**, *43*, 2080.
[20] V. K. Praveen, C. Ranjith, N. Armaroli, *Angew. Chem. Int. Ed.* **2014**, *53*, 365; *Angew. Chem.* **2014**, *126*, 373.
[21] Y. Lan, M. G. Corradini, R. G. Weiss, S. R. Raghavanc, M. A. Rogers, *Chem. Soc. Rev.* **2015**, *44*, 6035.
[22] C. Geiger, M. Stanescu, L. Chen, D. G. Whitten, *Langmuir* **1999**, *15*, 2241.
[23] X. Zhang, R. Lu, J. Jia, X. Liu, P. Xue, D. Xu, H. Zhou, *Chem. Commun.* **2010**, *46*, 8419.
[24] P. Rajamalli, E. Prasad, *Org. Lett.* **2011**, *13*, 3714.
[25] F. Rodríguez-Llansola, J. F. Miravet, B. Escuder, *Chem. Commun.* **2011**, *47*, 4706.
[26] P. Jana, S. Maity, S. K. Maity, P. K. Ghorai, D. Halder, *Soft Matter* **2012**, *8*, 5621.
[27] C. Ou, J. Zhang, X. Zhang, Z. Yang, M. Chen, *Chem. Commun.* **2013**, *49*, 1853.
[28] C. Zhao, B. Bai, H. Wang, S. Qu, G. Xiao, T. Tian, M. Li, *J. Mol. Struct.* **2013**, *1037*, 130.
[29] D. B. Rasale, I. Maity, A. K. Das, *Chem. Commun.* **2014**, *50*, 8685.
[30] N. Mizoshita, Y. Suzuki, K. Hanabusa, T. Kato, *J. Mater. Chem.* **2002**, *12*, 2197.
[31] K. Kato, S. Hayashi, *Develop. Growth Differ.* **2008**, *50*, 381.
[32] M. M. Frigault, J. Lacoste, J. L. Swift, C. M. Brown, *J. Cell Sci.* **2009**, *122*, 753.
[33] K. Hanabusa, K. Harano, M. Fujisaki, Y. Nomura, M. Suzuki, *Macromol. Symp.*, unpublished results.
[34] M. Suzuki, S. Owa, M. Kimura, A. Kurose, H. Shirai, K. Hanabusa, *Tetrahedron Lett.* **2005**, *46*, 303.
[35] S. Kobayashi, K. Hanabusa, N. Hamasaki, M. Kimura, H. Shirai, S. Shinkai, *Chem. Mater.* **2000**, *12*, 1523.
[36] K. Hanabusa, H. Fukui, M. Suzuki, H. Shirai, *Langmuir* **2005**, *21*, 10383.

Received: July 12, 2016
Published online on ■■ ■■, 0000

FULL PAPER

Supramolecular Chemistry

K. Hanabusa, T. Ueda, S. Takata, M. Suzuki*

■■ – ■■

Synthesis of Fluorescent Gelators and Direct Observation of Gelation with a Fluorescence Microscope

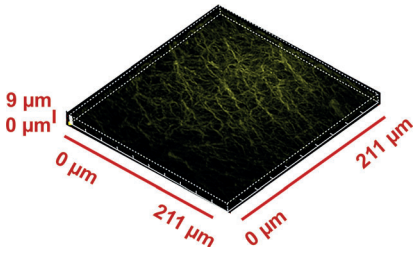

Loading image: A 3D image of a DMSO gel of a fluorescein-containing gelator was constructed by confocal laser scanning microscopy. The image was collected every 0.1 µm to a depth of 9 µm, resulting in a total of 90 images. The obtained 3D image of a 200×200 µm area is shown here. The large micrometer-size aggregates spread out three-dimensionally and the resulting 3D networks trap solvents in space, with gelation occurring as the final step.